www.elsevier.nl/locate/jorganchem

Journal of Organometallic Chemistry 611 (2000) 343–348

Journal of Organometallic Chemistry

Review

Structure and fluxional behavior of platinum and palladium complexes having M–Si or M–Sn (M = Pt or Pd) inter-element linkages

Yasushi Tsuji *, Yasushi Obora

Catalysis Research Center and Division of Chemistry, Graduate School of Science, Hokkaido University, Sapporo 060-0811, Japan

Received 1 March 2000; received in revised form 17 April 2000; accepted 18 April 2000

Abstract

Hexamethyldistannane reacts with $Pt\{P(MeC_6H_4)_3\}_4$ at $-30°C$ to afford the oxidative addition product: *cis*-$[Pt(SnMe_3)_2\{P(MeC_6H_4)_3\}_2]$. The structure is distinctly distorted from planarity: the dihedral angle between the P–Pt–P and the Sn–Pt–Sn planes is 34.6°. The solution ^{31}P-NMR spectra indicate that the complex shows reversible fluxional behavior. The fluxional process is attributed to the intramolecular twist-rotational motion via pseudo tetrahedral transition state. A similar fluxional process is observed with bis(silyl)bis(phosphine)platinum and bis(stannyl)bis(phosphine)palladium complexes. © 2000 Elsevier Science S.A. All rights reserved.

Keywords: Bis(stannyl)bis(phosphine)platinum; Bis(silyl)bis(phosphine)platinum; Bis(stannyl)bis(phosphine)palladium; Fluxional behavior; Active catalyst species

1. Introduction

Inter-element linkages of M–Si and M–Sn (M = transition metals) are highly important as active catalyst species in transition metal catalyzed silylation or stannylation reactions. In particular, organodistannanes (R_3SnSnR_3) [1] and disilanes (R_3SiSiR_3) [2] are good stannylating and silylating reagents in the presence of a transition metal complex as a catalyst. The first step in this catalysis is believed to be oxidative addition of a Sn–Sn or Si–Si σ-bond to the metal center to afford the inter-element linkages involving bis(stannyl) [3] or bis(silyl) metal species [4]. Here, we wish to review structures and fluxional behaviors of bis(stannyl)bis(phosphine)platinum (**1**), bis(silyl)bis(phosphine)platinum (**2**), and bis(stannyl)bis(phosphine)palladium complexes (**3**) (Chart 1). They all have twisted square planar structures and show facile unimolecular twist-rotation.

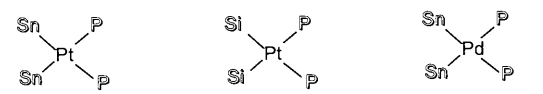

1 2 3

Chart 1.

2. Bis(stannyl)bis(phosphine)platinum complexes (1)

2.1. Molecular structure

A series of bis(stannyl)bis(phosphine)platinum complexes (**1a**, **1b**, **1c**) was obtained by oxidative addition of hexamethyldistannane (**4a**) to Pt(0) phosphine complexes such as **5a**, **5b**, and **5c** (Eq. (1)). Fig. 1 shows the molecular structure of **1b** determined by X-ray crystallographic analysis. The complex has twisted square-planar structure with *cis*-orientation of the ligands. The structure is distinctly distorted from planarity: the dihe-

* Corresponding author. Fax: +81-11-7062914.
E-mail address: tsuji@cat.hokudai.ac.jp (Y. Tsuji).

PII: S0022-328X(00)00449-6

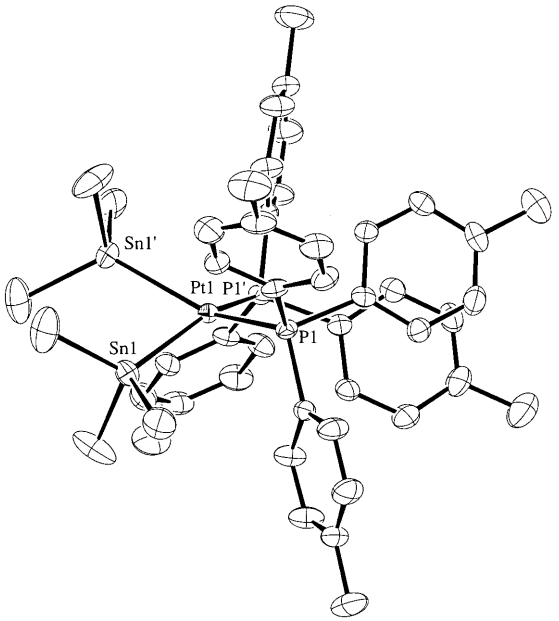

Fig. 1. Molecular structure of **1b**. Hydrogen atoms are omitted for clarity. The Pt atom is on a crystallographic twofold axis.

dral angle between the PtP_2 and the $PtSn_2$ planes is 34.6°.

$$Me_3SnSnMe_3 \ (\mathbf{4a}) + Pt(PR_3)_4 \longrightarrow Pt(SnMe_3)_2(PR_3)_2 \quad (1)$$

R_3 =		R_3 =	
5a: $(C_6H_5)_3$		**1a**: $(C_6H_5)_3$	91%
b: $(4\text{-}MeC_6H_4)_3$		**b**: $(4\text{-}MeC_6H_4)_3$	83%
c: $(C_6H_5)_2Me$		**c**: $(C_6H_5)_2Me$	70%

2.2. ^{31}P-NMR spectra and fluxional structure

Fluxionality of the resulting bis(stannyl)bis(phosphine)platinum complexes (**1**) was investigated with solution ^{31}P-NMR at various temperatures [5]. In Fig. 2a, a ^{31}P-NMR spectrum of **1b** measured at −90°C showed resonances centered at 32.2 ppm with satellite peaks due to $^1J_{P-Pt}$ (2645 Hz, not shown in the figure), $^2J_{P-Sn(transoid)}$ (1439 Hz with ^{117}Sn and 1507 Hz with ^{119}Sn), $^2J_{P-Sn(cisoid)}$ (181 Hz; peaks due to ^{117}Sn and ^{119}Sn were not resolved), and $^2J_{P-P}$ (13 Hz). Solid state CPMAS ^{31}P-NMR measured at room temperature (Fig. 2f) shows similar $^2J_{P-Sn(transoid)}$ (1500 Hz) and $^1J_{P-Pt}$ (2700 Hz, not shown in the figure) values, while $^2J_{P-Sn(cisoid)}$ coupling which is estimated to be ca. 180 Hz seems to be buried in the line width (300 Hz) of the main peak. It is clearly indicated by the solution NMR spectra that the complex shows reversible fluxional behavior. On warming, satellite peaks due to the two kinds of $^2J_{P-Sn}$ coalesced at −50°C (Fig. 2c) while maintaining the $^1J_{P-Pt}$ coupling (2644 Hz, not shown), and then sharpened at 20°C with the averaged $^2J_{P-Sn}$ (629 Hz with ^{117}Sn and 663 Hz with ^{119}Sn) (Fig. 2e). By analyzing the line width alternation, the thermodynamic parameters were obtained as follows: $\Delta H^{\ddagger} = 42 \pm 1$ kJ mol^{-1} and $\Delta S^{\ddagger} = 7.6 \pm 5.8$ J mol^{-1}K^{-1}. The rate of the fluxional process depended neither on concentration of **1b** (from 8.8 to 22 mol dm^{-3}) nor on the solvent employed, CD_2Cl_2 or $C_6D_5CD_3$. Furthermore, 1 M excess of $P(4\text{–}MeC_6H_4)_3$ added to **1b** did not affect the rate.

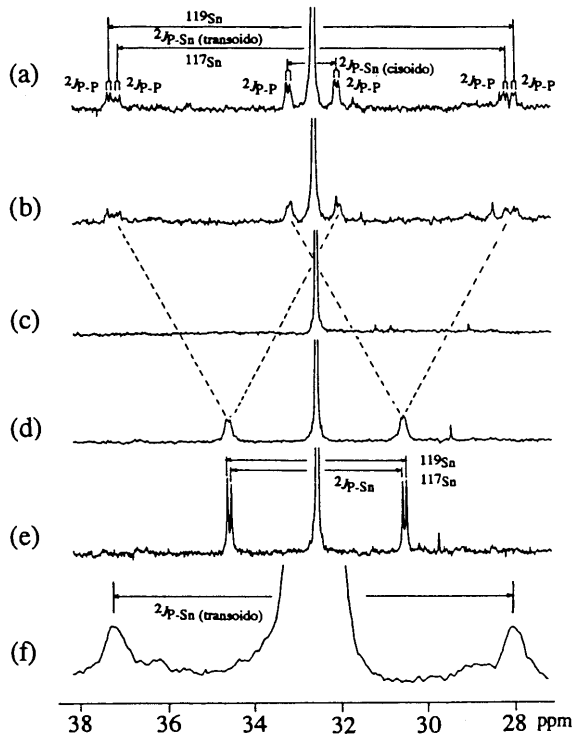

Fig. 2. Central part of ^{31}P-NMR spectra of **1b** (161.70 MHz). Solution NMR spectra measured in CD_2Cl_2 at (a) −90°C; (b) −80°C; (c) −50°C; (d) −10°C; (e) 20°C, and (f) CPMAS solid state NMR spectrum measured at room temperature. Chemical shifts are relative to H_3PO_4.

Among the bis(stannyl)bis(phosphine) complexes (**1a–c**), **1c** is a mixture of two isomers (*c*-**1c** and *t*-**1c** in 9:1 ratio), while **1a** and **1b** consist of a single isomer. All the products including **1c** showed good elementary analysis data. The $^2J_{P-Sn}$ values of **1a**, **1b**, and *c*-**1c** are similar (625–687 Hz), but that of *t*-**1c** is quite small in comparsion (169 and 176 Hz). The complex *c*-**1c** showed analogous fluxional behavior ($\Delta H^{\ddagger} = 60 \pm 1$ kJ mol^{-1} and $\Delta S^{\ddagger} = 32 \pm 5$ J mol^{-1} K^{-1}), in which satellite peaks due to $^2J_{P-Sn}$ coalesced at 2°C, and $^2J_{P-Sn(transoid)}$ (1482 Hz with ^{117}Sn and 1551 Hz with ^{119}Sn), $^2J_{P-Sn(cisoid)}$ (177 Hz), and $^2J_{P-P}$ (21 Hz) appeared at −50°C. These *J* values of *c*-**1c** are very close to those of **1b**. Therefore, *c*-**1c** was assigned to *cis*-$[Pt(SnMe_3)_2(PMePh_2)_2]$, while *t*-**1c** to the corresponding *trans*-isomer. Interestingly the *trans*-isomer *t*-**1c** did not show any fluxional behavior at all. The ratio between *c*-**1c** and *t*-**1c** (9:1) did not change after 1 week at room temperature, indicating no interconversion between *c*-**1c** and *t*-**1c.**

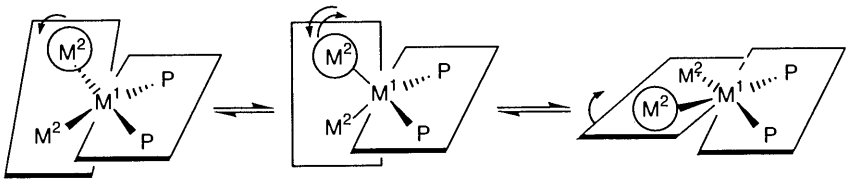

1: M^1 = Pt, M^2 = Sn
2: M^1 = Pt, M^2 = Si
3: M^1 = Pd, M^2 = Sn

Scheme 1.

Dissociative mechanisms for the fluxional process must be ruled out by the intramolecular conservation of the P and Sn nuclear spin states, which is shown by the sharp satellite peaks due to the $^1J_{P-Pt}$ and the line width alternation of the satellite peaks due to the $^2J_{P-Sn}$ in ^{31}P-NMR (Fig. 2a–e). Associative processes are also unlikely, since the concentration of the complex, the addition of excess phosphine, and the nature of the solvent did not affect the fluxional process (vide supra). The fluxional process must be attributed to the intramolecular twist-rotational motion via pseudo tetrahedral transition state (Scheme 1).

2.3. Ab initio molecular orbital calculation

Experimentally, it seems to be rather difficult to determine the origin of the fluxionality observed with **1**. Therefore, ab initio molecular orbital calculation was carried out with $Pt(SnH_3)_2(PtH_3)_2$ as a model complex [5]. The MP2-optimized geometry is planar. Thus, the distortion from planarity of **1b** may be attributed to the steric effect associated with the substituents on the P and the Sn atoms. The calculated activation energy of the fluxional process was 80.0 kJ mol^{-1}, which is consistent with the experimental values ($\Delta H^{\ddagger} = 42$ kJ mol^{-1} for **1b** and 60 kJ mol^{-1} for *c*-**1c**). In the calculated transition state, the P–Pt–P angle increased dramatically and electron density was considerably transferred from the Sn onto the Pt and the P, suggesting decrease of the activation energy by introduction of electron withdrawing substituents on the P atoms and increase of it by substitution of the Sn with a more electronegative element such as C.

3. Bis(silyl)bis(phosphine)platinum (2) and bis(stannyl)bis(phosphine)palladium complexes (3)

Ab initio molecular orbital calculations carried out for *cis*-$[Pt(SiH_3)_2(PH_3)_3]$ and *cis*-$[Pd(SnH_3)_2(PH_3)_2]$ as model compounds suggest that bis(silyl)bis(phosphine)platinum (**2**), and bis(stannyl)bis(phosphine)-palladium complexes (**3**) (Chart 1) have comparable activation energy for the similar twist-rotation as observed with **1** (Scheme 1). However, there were no reports on the fluxionality of **2** and **3**. Therefore, some representative complexes were prepared and characterized to elucidate the fluxionality.

3.1. Bis(silyl)bis(phosphine)platinum complexes (2)

cis-$[Pt(SiPh_2Me)_2(PMe_2Ph)_2]$ (**2a**) was prepared by the method reported by Chatt et al. [6] using the corresponding dichloroplatinum complex and the silyl lithium. An X-ray diffraction study was carried out, since no X-ray structure of **2a** was available. The molecular structure of **2a** is shown in Fig. 3. With *cis*-orientation of the ligands, the complex has a twisted square-planar structure. The structure is distinctly distorted from planarity; the dihedral angle between the PtP_2 and the $PtSi_2$ plane is 38.1°. As was the case with bis(stannyl)bis(phosphine)platinum complexes (**1**), the steric congestion associated with the substituents on the P and the Si atoms may cause the distortion from the planarity.

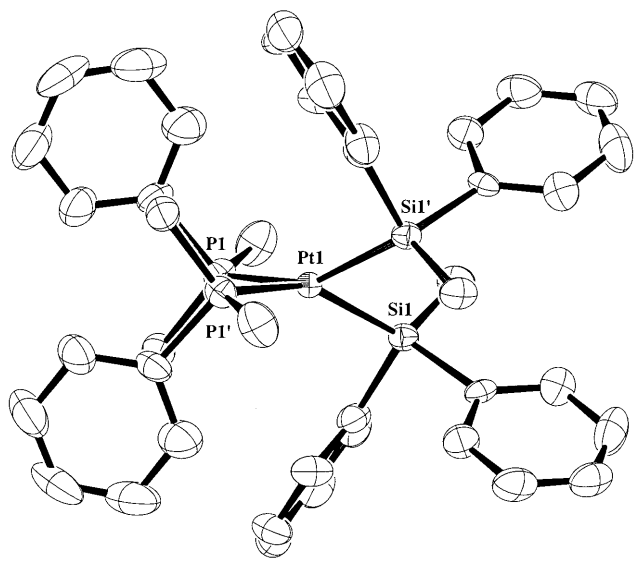

Fig. 3. Perspective ORTEP drawing of the molecular structure of complex **2a**. All non-hydrogen atoms are represented by thermal ellipsoids drawn to encompass 50% probability, and hydrogen atoms are deleted for ease of viewing.

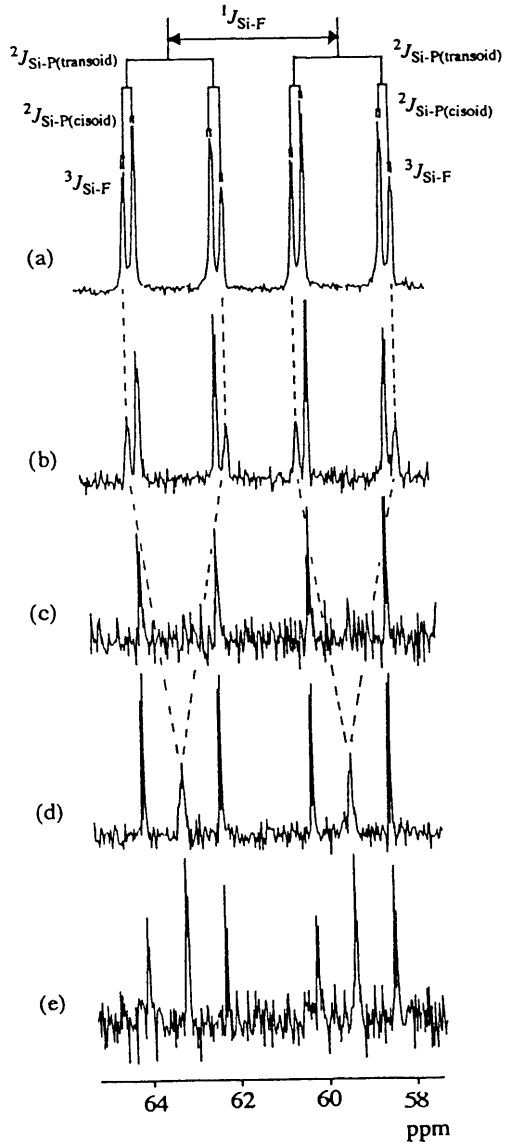

Fig. 4. ^{29}Si-NMR spectra (central part) of **2b** in toluene-d_8 (79.3 MHz) at (a) −80°C; (b) −50°C; (c) −30°C; (d) 20°C, and (e) 40°C.

At various temperatures the $^{31}P\{^1H\}$-NMR spectra of **2a** were measured [7]. The spectrum at −70°C showed the resonances centered at −7.8 ppm with the satellite peaks due to $^2J_{P-Si(transoid)}$ (156 Hz), $^2J_{P-Si(cisoid)}$ (18 Hz), and $^2J_{P-P}$ (24 Hz). On warming, the satellite peaks due to the $^2J_{P-Si(transoid)}$ and $^2J_{P-Si(cisoid)}$ became broad at −30°C and coalesced at −10°C while maintaining the sharp main resonance. The satellite peaks reappeared as the broad resonances at −10°C and sharpened at 30°C with the averaged $^2J_{P-Si}$ value (69 Hz). This fluxional process is reversible and throughout the process the $^1J_{P-Pt}$ is maintained; $^1J_{P-Pt} = 1572$ Hz at −70°C, 1570 Hz at −30°C, 1566 Hz at −10°C, 1560 Hz at 10°C, and 1557 Hz at 30°C. The thermodynamic parameters were obtained by simulating the spectra: $\Delta H^{\ddagger} = 57 \pm 2$ kJ mol^{-1} and $\Delta S^{\ddagger} = 17 \pm 9$ J mol^{-1} K^{-1}. *cis*-[Pt(SiFMe$_2$)$_2$(PEt$_3$)$_2$] (**2b**) also shows the distinct fluxional behavior. The fluxional process of **2b** was examined with $^{29}Si\{^1H\}$-NMR at various temperatures (Fig. 4) [7]. At −80°C (Fig. 4a), the resonances (61.2 ppm) appeared as two sets of ddd with $^1J_{Si-F}$ (300 Hz), $^2J_{Si-P(transoid)}$ (157 Hz), $^2J_{Si-P(cisoid)}$ (19 Hz), and $^3J_{Si-F}$ (3.9 Hz); satellite peaks due to $^1J_{Si-Pt}$ are omitted in the figure. At higher temperature, only the outer resonances of each set became broad at −50°C (Fig. 4b) and collapsed at −30°C (Fig. 4c). The resonances reappeared as the broad peaks at 20°C (Fig. 4d) and then sharpened at 40°C (Fig. 4e) at the midpoint of the resonances with $^1J_{Si-F}$ (302 Hz), $^2J_{Si-P}$ (69 Hz), and $^3J_{Si-F}$ (3.9 Hz). In the meantime, the inner lines remained sharp with the constant separation: $[|^2J_{Si-P(transoid)}| - |^2J_{Si-P(cisoid)}|]$. The inner lines are assigned to ^{29}Si transitions associated with the phosphorus spin states αα and ββ, while the collapsing (outer) lines to transitions with the phosphorus spin states αβ and βα. This behavior also indicates that the signs of the $^2J_{P-Si(transoid)}$ and $^2J_{P-Si(cisoid)}$ are opposite each other. The fluxional process is reversible and throughout the process the $^1J_{P-Pt}$ is maintained; $^1J_{P-Pt} = 1243$ Hz at −80°C, 1250 Hz at −50°C, 1252 Hz at −30°C, 1267 Hz at 20°C, and 1269 Hz at 40°C. By simulating the spectra, the following activation parameters were obtained: $\Delta H^{\ddagger} = 34 \pm 1$ kJ mol^{-1} and $\Delta S^{\ddagger} = -60 \pm 6$ J mol^{-1} K^{-1}.

As shown above, the spin–spin coupling between P, Si, and Pt nuclei are retained in these fluxional process of **2a** and **2b**; namely these nuclear spin states are intramolecularly conserved. Thus, within the limits of the NMR experiments, dissociative or consecutive displacement mechanisms involving Pt–Si or Pt–P bond cleavage can be excluded. Analogous fluxional behavior was observed for *cis*-[PtH(SiR$_3$)(PPh$_3$)$_2$] [8]. These features of the bis(silyl)platinum complexes (**2a**,**b**) are very reminiscent of the corresponding bis(stannyl)platinum complexes (**1**) [5]. Ab initio molecular orbital calculations carried out for *cis*-[Pt(SiH$_3$)$_2$(PH$_3$)$_2$] as a model complex suggest that **2** and **1** have comparable activation energy for the twist-rotation, which is supported by the observed $\Delta H^{\ddagger}$ values for **2a** and **2b** (vide supra). Thus, we attribute the fluxionality of **2a** and **2b** to the similar unimolecular twist-rotation via pseudo tetrahedral transition state (Scheme 1).

3.2. Bis(stannyl)bis(phosphine)palladium complexes (3)

The oxidative addition of Me$_3$SnSnMe$_3$ (**4a**) to the palladium(0) phosphine complexes (**6a** and **6b**) [9] affords the corresponding new *cis*-bis(stannyl)bis(phosphine)palladium complexes (**3a** and **3b**) as analytically pure forms (Eq. (2)). It is noteworthy that this is the first example of the oxidative addition of a Sn–Sn σ-bond to a palladium(0) phosphine complex

which is often employed as a catalyst precursor in the bis-stannylation reaction using organodistannanes. X-ray crystallographic analysis was carried out for trimethylphosphine complex (**3a**) and the molecular structure was shown in Fig. 5. Again, the complex has a twisted square-planar structure; the dihedral angle between the PdP_2 and the $PdSn_2$ plane is 16.8°.

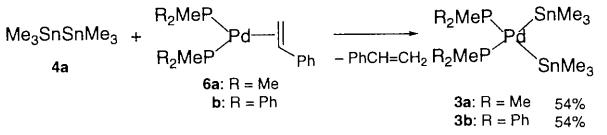

(2)

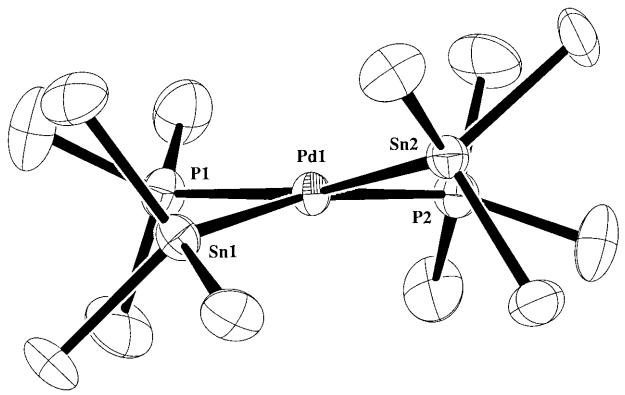

Fig. 5. Perspective ORTEP drawing of the molecular structure of complex **3a**. All non-hydrogen atoms are represented by thermal ellipsoids drawn to encompass 50% probability, and hydrogen atoms are deleted for ease of viewing.

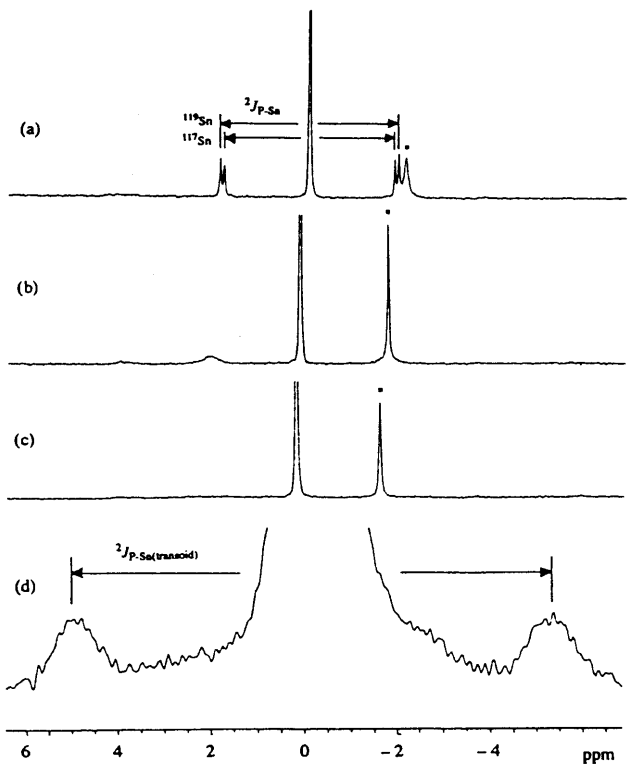

Fig. 6. ^{31}P-NMR spectra (central part) of **3b** in toluene-d_8 (162 MHz) at (a) −50°C; (b) −80°C; (c) −90°C, and (d) solid-state CPMAS spectrum (162 MHz) at 25°C.

In the $^{31}P\{^1H\}$-NMR spectra of **3a**, ^{31}P resonances appeared as a sharp peak at −28.0 ppm (at −90°C), while at room temperature the resonances were broad (line width at half height: 100 Hz) without any J couplings. Although the complex was analytically pure, two large unidentified resonances appeared at −34.6 and −21.5 ppm having some J_{P-P} and J_{P-Sn} couplings; the ratio of the resonances at −34.6, −28.0, and −21.5 ppm is 1:1:1 at −90°C. Since a $^{119}Sn\{^1H\}$-NMR spectrum of the same solution confirmed a comparable formation of $Me_3SnSnMe_3$ (−110.40 ppm, $^1J_{Sn-Sn} = 4165$ Hz; lit. [10]: −108.7 ppm, $^1J_{Sn\text{-}Sn} = 4210$ Hz), the unidentified resonances may be assigned to a species formed by reductive elimination giving $Me_3SnSnMe_3$. Addition of two equivalents of $Me_3SnSnMe_3$ to the solution reduced the unidentified resonances at −34.6 and −21.5 ppm and enhanced the resonance of **3a** (−28.0 ppm); the ratio between these resonances became 1:9:1 at −90°C. Irrespective of absence or presence of the added $Me_3SnSnMe_3$, the resonance of **3a** at −28.0 ppm has $^2J_{P-Sn(transoid)}$ (1546 and 1618 Hz), $^2J_{P-Sn(cisoid)}$ (203 Hz), and $^2J_{P-P}$ (38 Hz) couplings, which is consistent with the static *cis*-structure such as shown in Fig. 5.

Methyldiphenylphosphine complex (**3b**) was prepared (Eq. (2)) and characterized because fluxional behavior was not explicit with **3a**. In contrast to **3a**, **3b** does not undergo the reductive elimination giving $Me_3SnSnMe_3$ judging from $^{119}Sn\{^1H\}$-NMR. Therefore, $^{31}P\{^1H\}$-NMR of **3b** is fairly simple even without the added $Me_3SnSnMe_3$, although the small unidentified peak appeared. The ^{31}P resonance measured at −50°C (Fig. 6a) has satellite peaks due to $^2J_{P-Sn}$ (596 and 623 Hz). Since the $^2J_{P-Sn}$ values are comparable to $(|^2J_{Sn-P(transoid)}| - |^2J_{Sn-P(cisoid)}|)/2$ calculated for **3a** (namely, 672 and 708 Hz: the averaged $^2J_{P-Sn}$ values), it is evident that **3b** undergoes fluxional process and the process is fast on the NMR time-scale even at −50°C. With lowering of the temperature, the satellite peak became broad at −80°C (Fig. 6b) and coalesced at −90°C (Fig. 6c) while maintaining the sharp main resonance. The fluxional process could not be frozen in the solution state because of the solvent freezing and limited solubility of the complex in other solvents of lower freezing point. However, solid state CPMAS $^{31}P\{^1H\}$-NMR measured at 25°C (Fig. 6d) revealed the static *cis*-structure of **3b**. In the spectrum, the satellite peak due to $^2J_{P-Sn(transoid)}$ (1650 Hz) appeared with a similar J value to those of **3a** (1546 and 1618 Hz, vide supra), whereas $^2J_{P-Sn(cisoid)}$ coupling (203 Hz for **3a**) may be buried in the broad main peak (line width at half height: 300 Hz). Thus, the fluxional behavior of **3b** is evident by utilizing both solution and solid state ^{31}P-NMR. The fluxional process of **3b** in which the P and Sn spin states are conserved may be explained

analogously by the unimolecular twist rotation depicted in Scheme 1 (see Fig. 6).

Acknowledgements

The authors are grateful to Professor Takashi Kawamura of Gifu University for ab initio molecular orbital calculation and helpful discussion, and to Professor Masahiro Ebihara of Gifu University for X-ray crystallographic analysis.

References

[1] (a) Y. Obora, Y. Tsuji, T. Kakehi, M. Kobayashi, Y. Shinkai, M. Ebihara, T. Kawamura, J. Chem. Soc. Perkin Trans. 1 (1995) 599. (b) Y. Tsuji, T. Kakehi, J. Chem. Soc. Chem. Commun. (1992) 1000. (c) E. Piers, R.T. Skerlj, J. Chem. Soc. Chem. Commun. (1986) 626. (d) T.N. Mitchell, A. Amamria, H. Killing, D. Rutschow, J. Organomet. Chem. C45 (1983) 241.

[2] (a) Y. Tsuji, M. Funato, M. Ozawa, H. Ogiyama, S. Kajita, T. Kawamura, J. Org. Chem. 61 (1996) 5779. (b) Y. Obora, Y. Tsuji, T. Kawamura, J. Am. Chem. Soc. 117 (1995) 9814. (c) Y. Obora, Y. Tsuji, T. Kawamura, J. Am. Chem. Soc. 115 (1993) 10414. (d) Y. Tsuji, S. Kajita, S. Isobe, M. Funato, J. Org. Chem. 58 (1993) 3607. (e) Y. Tsuji, R.M. Lago, S. Tomohiro, H. Tsuneishi, Organometallics 11 (1992) 2353. (f) M. Murakami, M. Sugimome, K. Fujimoto, H. Nakamura, P.G. Anderson, Y. Ito, J. Am. Chem. Soc. 115 (1993) 6487. (g) Y. Ito, M. Suginome, M. Murakami, J. Org. Chem. 56 (1991) 1948. (h) H. Yamashita, M. Catellani, M. Tanaka, Chem. Lett. (1991) 241. (i) H. Sakurai, Y. Eriyama, Y. Kamiyama, Y. Nakadaira, J. Organomet. Chem. 264 (1984) 229. (j) H. Watanabe, M. Kobayashi, M. Saito, Y. Nagai, J. Organomet. Chem. 216 (1981) 149. (k) H. Watanabe, M. Kobayashi, K. Higuchi, Y. Nagai, J. Organomet. Chem. 186 (1980) 51. (l) H. Matsumoto, I. Matsubara, T. Kato, K. Shono, H. Watanabe, Y, Nagai, J. Organomet. Chem. 199 (1980) 43. (m) H. Matsumoto, K. Shono, A. Wada, I. Matsubara, H. Watanabe, Y. Nagai, J. Organomet. Chem. 199 (1980) 185. (n) K. Tamao, S. Okazaki, M. Kumada, J. Organomet. Chem. 146 (1978) 87. (o) K. Tamao, T. Hayashi, M. Kumada, J. Organomet. Chem. 114 (1976), C19. (p) H. Sakurai, Y. Kamiyama, Y. Nakadaira, Chem. Lett. (1975) 887. (q) H. Sakurai, Y. Kamiyama, Y. Nakadaira, J. Am. Chem. Soc. 97 (1975) 931. (r) H. Okinoshima, K. Yamamoto, M. Kumada, J. Am. Chem. Soc. 94 (1972) 9263.

[3] (a) M. Akhtar, H.C. Clark, J. Organomet. Chem. 22 (1970) 233. (b) H.J. Weichmann, Organomet. Chem. 238 (1982) C49.

[4] (a) F. Ozawa, J. Kamite, Organometallics 17 (1998) 5630. (b) F. Ozawa, M. Sugawara, T. Hayashi, Organometallics 13 (1994) 3237. (c) H. Yamashita, T. Kobayashi, T. Hayashi, M. Tanaka, Chem. Lett. (1990) 1447. (d) M. Suginome, H. Oike, S.-S. Park, Y. Ito, Bull. Chem. Soc. Jpn. 69 (1996) 289.

[5] Y. Obora, Y. Tsuji, K. Nishiyama, M. Ebihara, T. Kawamura, J. Am. Chem. Soc. 118 (1996) 10922.

[6] (a) J. Chatt, C. Eaborn, S.D. Ibekwe, P.N. Kapoor, J. Chem. Soc. (A) (1970) 1343. (b) C. Eaborn, T.N. Metham, A. Pidcock J. Chem. Soc. Dalton Trans. (1975) 2212. (c) C. Eaborn, A. Pidcock, B. Ratcliff, J. Organomet. Chem. 66 (1974) 23.

[7] Y. Tsuji, K. Nishiyama, S. Hori, M. Ebihara, T. Kawamura, Organometallics 17 (1998) 507.

[8] H. Azizian, K.R. Dixon, C. Eaborn, A. Pidcock, N.M. Shuaib, J. Vinaixa, J. Chem. Soc. Chem. Commun. (1982) 1020.

[9] F. Ozawa, T. Son, S. Ebina, K. Osakada, A. Yamamoto, Organometallics 11 (1992) 171 and references therein.

[10] T.N. Mitchell, G. Walter, J. Chem. Soc. Perkin Trans. 2 (1997) 1842.